THE ASTROPHYSICAL JOURNAL, 473:963–973, 1996 December 20

LUMINOSITY DIFFERENCES BETWEEN BLACK HOLES AND NEUTRON STARS

DIDIER BARRET,[1,2] JEFFREY E. MCCLINTOCK,[3] AND JONATHAN E. GRINDLAY[4]
Harvard Smithsonian Center for Astrophysics, 60 Garden Street, Cambridge, MA 02138
Received 1996 March 18; accepted 1996 June 12

ABSTRACT

We compare the X-ray (1–20 keV) and hard X-ray (20–200 keV) luminosities of black hole binaries (BHBs; i.e., binaries for which the mass of the compact object is known to exceed 3 $M_\odot$) and X-ray bursters (neutron star binaries, NSBs). We discuss two ways of distinguishing a BHB from a NSB: (1) If the X-ray luminosity exceeds $\sim 10^{37}$ ergs s^{-1}, the hard X-ray luminosity of BHBs is relatively unaffected, whereas the hard X-ray luminosity of NSBs decreases drastically; and (2) the hard X-ray luminosity of BHBs is commonly in the range 10^{37}–6×10^{37} ergs s^{-1}, whereas for NSBs it is $\lesssim 10^{37}$ ergs s^{-1}. We show that late in their decays transient BHBs (e.g., GRS 1124−68) have X-ray and hard X-ray luminosities comparable to those observed for NSBs. Thus BHBs can be distinguished from NSBs only at relatively high luminosities.

We also compare NSBs with the so-called black hole candidates (BHCs; i.e., systems with similar spectral/temporal properties to BHBs). The X-ray and hard X-ray luminosities of LMC X-1, GRO J0422+32, GRS 1915+105, 4U 1543−47, and 4U 1630−47 are much larger than the maximum luminosities observed from NSBs, which supports the idea that they contain black holes. Three other BHCs, namely GRS 1716−249, 1E 1740.7−2942, and GRS 1758−258 (which all lack an ultrasoft spectral component), have hard X-ray luminosities at least a factor of $\sim$2–3 above the maximum observed from NSBs, which suggests that these objects also contain black hole primaries. The case of GX 339−4 remains very uncertain because of the large uncertainty in its distance estimates (from 1.3 to 4 kpc). Assuming the larger distance, the X-ray and hard X-ray luminosities of the source, and its luminosity-related spectral changes which are similar to transient BHBs (e.g., GRS 1124−68), support the idea that it contains a black hole. Finally, the X-ray and hard X-ray luminosities of the puzzling X-ray source 4U 1957+11 are in the range of those observed for NSBs, consistent with the idea that it might contain a neutron star. If 4U 1957+11 is, in fact, a neutron star system, this would establish that the combination of a power-law tail and an ultrasoft component (which is present in the spectrum of 4U 1957+11) is not a unique spectral signature of an accreting black hole.

Subject headings: black hole physics — stars: neutron — X-rays: general — X-rays: stars

1. INTRODUCTION

The best evidence for the presence of a black hole (BH) in an X-ray binary is a measurement of the mass function that establishes a lower limit of $\sim 3\ M_\odot$ on the mass of the compact object (van Paradijs & McClintock 1995). To date six such systems have been discovered, namely the soft X-ray transients A0620−00, GRS 1124−68, GRO J1655−40, H1705−250, GS 2000+250, and GS 2023+338 (see Table 1 for system parameters and references). Unfortunately, a determination of the mass function is not always possible. For example, an object may be too distant or too reddened or have an accretion disk that is persistently too bright. Indeed, for the six transient sources listed above, the mass function estimates have been determined in quiescence, when their low-mass secondary star dominates the optical emission. Thus, it is important to search for X-ray/hard X-ray emission properties (temporal and spectral) that may be unique to BH systems or at least commonly associated with BH systems. Unfortunately, over the past 20 years essentially all of the BH signatures that have been proposed (e.g., rapid X-ray variability) were subsequently observed in certain neutron star (NS) systems (e.g., Tanaka & Lewin 1995; van der Klis 1994). Among these BH signatures, a power law tail (also "hard tail") extending up to hard X-ray energies ($E \gtrsim 100$ keV) is currently believed to be the most secure (Sunyaev et al. 1991a; Grebenev et al. 1993). Recently hard X-ray tails have been observed also from several X-ray bursters (i.e., NS systems), casting doubts on the usefulness of this criterion for identifying black holes (Barret & Vendrenne 1994; Gilfanov et al. 1993a; Goldwurm et al. 1995; Barret & Grindlay 1996). The hard tail in the spectrum of an accreting neutron star, however, appears to be present only at relatively low luminosities (Barret & Vedrenne 1994). van Paradijs & van der Klis (1994) later suggested, using archival *HEAO 1* A-4 data, that unless we know that a system has a luminosity larger than $\sim 10^{37}$ ergs s^{-1}, the presence of a hard X-ray tail alone is not sufficient to claim that the system contains a black hole. However, they did not comment on the importance of the luminosity in the hard X-ray band, which is a major theme of this paper.

Although the diversity of spectral behavior observed from BH and NS systems clearly complicates the task of finding unabiguous criteria, there may still be some X-ray properties unique to BH systems: for example, the combination of an ultrasoft component[5] and a power-law tail (While 1993), or spectral differences between BH and NS

[1] Also Centre d'Etude Spatiale des Rayonnements, 9 Av du Colonel Roche, 31029 Toulouse, Cedex, France.
[2] dbarret@cfa.harvard.edu.
[3] jmcclintock@cfa.harvard.edu.
[4] jgrindlay@cfa.harvard.edu.

[5] An ultrasoft component has roughly a bremsstrahlung shape with a kT of $\sim$1–2 keV and dominates the X-ray spectrum below $\sim$10 keV (White 1993).

TABLE 1

MASS AND DISTANCE ESTIMATES FOR BLACK HOLE BINARIES

Object	P (hr)	i (deg)	M_1 ($M_\odot$)	M_1/M_2	R_2 ($R_\odot$)	$V_{0,2}$	Spectral Type	d (kpc)	References
Cyg X-1	134	35	10	0.57	17.3	5.6	O9.7 I_{ab}	1.9	1, 2, 3
LMC X-3	40.9	...	9	...	...	...	...	50	4, 5
A0620−00	7.75	55	6.1	14.0	0.70	17.8	K5	1.2[1.2]	6, 7, 8, 9
GRS 1124−68	10.4	60	6.0	7.5	1.03	20.3	K4	6.5[5.1]	10
GRO J1655−40	62.7	...	4.5	...	...	...	...	3.2	11, 12
H1705−250	12.5	60	7.5	12	1.08	20.5	K3	8.6[7.3]	13
GS 2000+250	8.26	66	7.2	20	0.68	19.6	K5	2.7[2.8]	14, 15
GS 2023+338	155	...	12	...	...	...	...	3.0	16

NOTE.—P: orbital period (hours); i: inclination (degrees); M_1: mass of the primary; M_1/M_2: mass ratio; R_2: radius of the secondary (in units of solar radius); $V_{0,2}$: dereddened apparent magnitude of the secondary star; Spectral Type: spectral type of the secondary. The distances in brackets are computed with "method II" (see text).

REFERENCES.—(1) Gies & Bolton 1982; (2) Gies & Bolton 1986; (3) Herrero et al. 1995; (4) Cowley et al. 1983; (5) Westerlund 1991; (6) Orosz et al. 1994; (7) Marsh et al. 1994; (8) Haswell et al. 1993; (9) Shahbaz et al. 1994a; (10) Orosz et al. 1996; (11) Bailyn et al. 1995; (12) Hjellming & Rupen 1995; (13) Remillard et al. 1996; (14) Filippenko et al. 1995a; (15) Casares et al. 1995a; (16) Shahbaz et al. 1994b.

systems due to differences at the inner disk radius (Tanaka & Lewin 1995), or the photon index of the power-law tail (Goldwurm et al. 1995), or the break/cutoff energy of the hard X-ray tail (Barret & Grindlay 1996).

In this paper, we compare the X-ray (1–20 keV) and hard X-ray (20–200 keV) luminosities (L_X vs. L_{HX}) of three classes of accreting sources: the black hole binaries (hereafter BHBs), the neutron star binaries (hereafter NSBs), and the black hole candidates (hereafter BHCs). Our objective is to establish differences between the BHBs and NSBs, which do not depend on the results of a detailed spectral analysis, and to use these differences to test the BHCs.

By BHBs we mean those systems for which there is very strong dynamical evidence that the primary is a black hole. Specifically, the BHBs comprise the six soft X-ray transients listed above plus the two high-mass X-ray binaries Cyg X-1 and LMC X-3 (see Table 1).

We select only NSBs for which a hard X-ray tail has been detected up to at least 100 keV. They are all type I X-ray burst sources, which establishes that their compact objects are NSs. The NSBs are listed in Table 2, together with their distance estimates which are based on an association with a globular cluster (e.g., SLX 1732−304 with Terzan 1), or on an optical study (e.g., 4U 0614+09), or on an X-ray burst study (e.g., 4U 1608−52). In particular, we are confident about the distances to Cen X-4, GX 354−0, 1E 1724−3045, and 4U 1608−52, since these sources show saturated X-ray bursts with photospheric radius expansion, which appears to be associated with an Eddington-limited burst luminosity (Lewin, van Paradijs, & Taam 1993). The distances to Cen X-4, 4U 1608−52, GX 354−0, and Aql X-1 can be compared with those given in van Paradijs & White (1995). Their distances are systematically larger (by an average ratio of 1.3) than the ones listed in Table 2, suggesting that the discrepancies are probably caused by differences in the assumptions made in the analysis.

Finally, we consider what we call the BHCs, systems such as LMC X-1, GX339−4, and 1E 1740.7−2942. These sources are BHCs based on their spectral/temporal properties, but convincing dynamical measurements have not yet been made. We have included all the BHCs listed in Tanaka

TABLE 2

DISTANCE ESTIMATES FOR NEUTRON STAR BINARIES

Object	d (kpc)	Comments	References
4U 0614 + 09	2.5	X-ray bursts and optical	1, 2
Cen X-4	1.2	X-ray bursts[a]	3
4U 1608−52	3.6	X-ray bursts[a]	4
4U 1705−44	7.4	X-ray bursts	5
1E 1724−3045	7.0	GC and X-ray bursts[a]	6
GX 354−0	5.7	X-ray bursts[a]	7
KS 1731−260	5.0[b]	X-ray bursts	8
SLX 1732−304	4.5	GC	9
A1742−294	8.5[b]	X-ray bursts	10
Aql X-1	2.5	Optical	11

NOTE.—GC: globular cluster.

[a] X-ray burst showing photospheric radius expansion.

[b] Uncertain.

REFERENCES.—(1) Brandt et al. 1993; (2) Machin et al. 1991; (3) Chevalier et al. 1989; (4) Nakamura et al. 1989; (5) Haberl & Titarchuk 1995; (6) Grindlay 1978; (7) van Paradijs 1978; (8) Barret & Grindlay 1996; (9) Ortolani, Bica, & Barbuy 1993; (10) Pavlinsky, Grebenev, & Sunyaev 1994; (11) Thorstensen, Charles, & Bowyer 1978.

TABLE 3

DISTANCE ESTIMATES FOR BLACK HOLE CANDIDATES

Object	d (kpc)	References
GRO J0422+32	3.6	1, 2, 3
LMC X-1	50.0	4, 5
GRS 1009−45	?	
GS 1354−64	?	
A1524−62	4.4	6
4U 1543−47	4.0	7
4U 1630−47[a]	10.0	8
GX 339−4	4.0	9
GRS 1716−249	2.4	10
KS 1730−312	?	
1E 1740.7−2942[b]	8.5	11
H1743−322	?	
X1755−338	9.0	12
GRS 1758−258[b]	8.5	13
GS 1826−24	?	
EXO 1846−031[a]	7.0	14
GRS 1915+105	12.5	15
4U 1957+11	7.0	16

[a] The distance is computed so that the X-ray luminosity at the peak of the outburst was $\sim 10^{38}$ ergs s^{-1}.

[b] Assumed to be at the Galactic center.

REFERENCES.—(1) Filippenko et al. 1995b; (2) Casares et al. 1995b; (3) Orosz & Bailyn 1995; (4) Hutchings et al. 1987; (5) Westerlund 1991; (6) van Paradijs & Verbunt 1984; (7) Chevalier 1989; (8) White et al. 1984; (9) Cowley et al. 1987; (10) Della Valle et al. 1994; (11) Grebenev et al. 1995; (12) Mason, Parmar, & White 1985; (13) Gilfanov et al. 1993b; (14) Parmar et al. 1993; (15) Chaty et al. 1996; (16) Margon, Thorstensen, & Bowyer 1978.

& Lewin (1995) plus three recently discovered sources: GRS 1009−45, GRS 1716−249, and KS 1730−312. The BHCs are listed in Table 3. Unfortunately for five of them, we could not find any distance estimates in the literature. For these objects, we will assume a plausible range of distances (5–10 kpc, see below).

In the following sections we discuss each of the three classes of objects and provide details on the X-ray and hard X-ray observations. We have selected simultaneous X-ray/hard X-ray observations whenever possible. We note that the hard X-ray fluxes observed from NSBs are fluxes recorded during hard X-ray outbursts, and hence probably close to the maximum these sources can reach. Therefore for consistency in the comparison, when several observations of BHBs or BHCs were available, we have always selected the ones associated with the largest hard X-ray fluxes.

2. THE BLACK HOLE BINARIES (BHBs)

Before discussing the BHB observations used in this paper, let us first make some comments on the distance and mass estimates given in Table 1. For Cyg X-1, LMC X-3, GRO J1655−40, and GS2023+338, we have adopted the distances and masses given in the literature. For the four remaining systems, we have used the data in the references cited to derive distances as follows. The dereddened magnitudes of the secondary stars ($V_{0,2}$) were obtained or derived from the references cited in the table. They take into account a correction for interstellar reddening and a correction for the continuum flux that is contributed by the accretion disk (e.g., Remillard et al. 1996). We used the available dynamical data, which are summarized in Table 1, to derive distances that are independent of any assumptions about the secondary star. We refer to this approach as "method I." First, we adopted a specific dynamical model for each system, which is based on the orbital period and the mass function, and also on two less certain parameters: the mass ratio (M_1/M_2) and the orbital inclination angle (i). We then computed the two masses (M_1 and M_2), their separation (via Kepler's law), and the Roche lobe radius of the secondary (Paczyński 1971), which we assume is the same as the radius of the secondary (R_2). Using visual absolute fluxes, which depend only on spectral type, we computed the absolute visual magnitude of the secondary (Popper 1980). Finally, using the apparent dereddened magnitude of the secondary ($V_{0,2}$) and the absolute magnitude, we obtained an estimate of the distance, which is given in Table 1 without brackets; these are the distances we have adopted for use in this paper. In most cases, the uncertainty in this distance estimate is primarily due to the uncertainty in the inclination angle i. As an example, consider the model for A0620−00 with $i = 55°$, which is summarized in Table 1. If i were increased to 65°, the distance would be decreased by 10%; on the other hand, if i were decreased to 45°, the distance would be increased by 16%.

We have also estimated the distances to the four sources in Table 1 in a second way, which we refer to as "method II." We obtained the radii of the secondary stars (R_2) using the relation for the average density of a Roche lobe–filling star, which is determined solely by the orbital period (Frank, King, & Raine 1992):

$$\rho \equiv \frac{3M_2}{4\pi R_2^3} \approx 115/P^2(\mathrm{hr})\ g\ \mathrm{cm}^{-3}\ .$$

For this method we must assume a value for the mass of the secondary star. For all four systems, which contain mid-K secondaries, we assume $M_2 = 0.4\ M_\odot$. This is a plausible value, and is very probably correct to within a factor of 2 (e.g., van Paradijs & McClintock 1994). Moreover, since d scales as $M_2^{1/3}$, the distances should be uncertain by only about ±25%. With the values of R_2 derived in this way, we computed the absolute magnitudes of the secondaries as before. Then, using the apparent dereddened magnitudes, we derived the distances that are enclosed in brackets in Table 1. For the two systems with $P_{\mathrm{orb}} \approx 8$ hr, A0620−00 and GS 2000+250, the distances obtained by the two methods are the same within ∼5%. However, for the systems with longer orbital periods (10.4 hr and 12.5 hr), GRS 1124−68 and H1705−250, method II gives distances that are less by ∼15% and 21%.

It is interesting to note that the average distance of the seven Galactic BHBs (i.e., excluding LMC X-3) is 3.9 kpc (with method I). This value is significantly lower than the Galactic center distance (8.5 kpc), which suggests that we are currently observing the relatively nearby systems and that indeed searches for fainter BHBs (e.g., as faint transients–see Grindlay et al. 1996) are likely to be rewarding.

In Table 4, we list the X-ray and hard X-ray spectral parameters and fluxes for the eight BHBs. Simultaneous observations exist for all the BHBs with the exception of LMC X-3, which is very faint in the hard X-ray band. Cyg X-1 was observed simultaneously by *Granat* in its standard "low" state (Grebenev et al. 1993). No "high" state data exist because the source has been observed only in the "low" state during the past 20 yr. (See Ubertini et al. 1991; Oda 1977; and Liang & Nolan 1984 for reviews of early observations of the source. See also Crary et al. 1996 and Philips et al. 1996 for recent observations of a super low state in hard X-rays which may correspond to a very high state in X-rays.)

We used the results of broadband observations of the transient BHBs that occurred closest to the time of X-ray maximum (the times of the observations compared to the X-ray maximum are given in the note to Table 4). The values of L_X presented herein are within a factor of ∼10 of the maximum X-ray luminosities reached by the sources (Tanaka & Lewin 1995).

The case of A0620−00 (Nova Mon 1975) is more complicated. The presence of a hard tail in the X-ray spectrum of this source is strongly suggested by the *OSO 8* data (White, Kaluzienski, & Swank 1994). In addition, two marginal detections of a weak hard tail extending up to ∼100 keV were reported by the *Ariel V* group (Coe, Engel, & Quenby 1976). On the other hand, observations made using *SAS 3* at comparable energies on three occasions yielded no detections (Cooke et al. 1984); however, these observations were not contemporaneous with the *OSO 8* and *Ariel V* observations. As for the *SAS 3* data, it is puzzling that the source was not detected between 8 and 35 keV, a band that includes a substantial contribution from the bright ultrasoft component. Possibly these nondetections at higher energies are due to the relative faintness of the source and/or to the observed spectral variability of BHBs (e.g., GRS 1124−68, see below). In any case, we have chosen to include A0620−00 in our comparison despite the controversy over the detection of hard X-rays (Tanaka & Lewin 1995).

TABLE 4

X-RAY TO HARD X-RAY OBSERVATIONS OF BLACK HOLE BINARIES

Object	Date	Experiments	Range (keV)	US[a] (Y/N)	Model	Parameters	F_X (ergs cm^{-2} s^{-1})	F_{HX} (ergs cm^{-2} s^{-1})	References
Cyg X-1	1990 Apr 23	ART-P and SIGMA	3–300	N	PL[b]/S&T	1.57, 57, 2.1	1.7×10^{-8}	3.9×10^{-8}	1
LMC X-3	1989 Mar 2	TTM	2–30	Y	D + PL[c]	28(50), 1.16, 2.3	1.5×10^{-9}	1.8×10^{-10}	2
A0620−00.....	1975 Aug 20–23	*Ariel V* (SSE and ST)	1–200	Y	PL + PL	4.7, 2.0	2.1×10^{-6}	3.7×19^{-9}	3
GRS 1124−68	1991 Jan 16	*Ginga* & SIGMA	1–300	Y	D + PL	10.5(1), 0.92, 2.3	1.8×10^{-7}	7.4×10^{-9}	4, 5
GRO J1655−40...	1995 Aug 16	ASCA and BATSE	1–200	Y	TB + PL	1.0, 2.3	6.8×10^{-8}	1.4×10^{-8}	6
H1705−250	1977 Sep 4–18	*HEAO* 1 A2 and A4	2–200	Y	TB + PL	1.8, 2.29	2.8×10^{-8}	5.3×10^{-9}	7
GS 2000+250	1988 May 15	*Kvant*	4–300	Y	TB + TB	1.99, 95	3.4×10^{-7}	5.7×10^{-9}	8
GS 2023+338	1989 Jun 10	*Kvant*	2–300	N	BPL	1.28, 2.14, 61.0	1.4×10^{-8}	3.4×10^{-8}	9

NOTE.—For A0620−00, the observation took place 1 week after the peak of the outburst, for GRS 1124−68 (1 week), H1705−250 (2 weeks), GS 2000+250 and GS 2023+338 (3 weeks). Range defines the energy range of the observations. Models (parameters) are: PL = power law (α: photon index), TB = thermal bremsstrahlung (kT: temperature), S&T = Sunyaev and Titarchuk Comptonization model (kT_e: electron temperature and τ: half optical thickness of the disk), BPL = broken power law (α_1, α_2: photon index and E_{Break}: energy of the break). D = multi-color blackbody disk model ($R_{in} \times \cos\theta^{1/2}$: inner disk radius given [the value in parenthesis is the distance at which the radius is given] and T_{in}: inner disk temperature). F_X and F_{HX} are the 1–20 keV and 20–200 keV fluxes derived from the best fit parameters.

[a] Indicates the presence of an ultrasoft component in the spectrum.

[b] The spectrum in the 3–30 keV band is independently fitted by a power law.

[c] The hard X-ray flux is extrapolated from the power-law tail observed in X-rays by TTM.

REFERENCES.—(1) Grebenev et al. 1993; (2) Pan et al. 1995; (3) Coe et al. 1976; (4) Ebisawa et al. 1994; (5) Goldwurm et al. 1992; (6) Zhang et al. 1996a; (7) Wilson & Rotschild 1983; (8) Sunyaev et al. 1988; (9) Sunyaev et al. 1991b.

TABLE 5

X-RAY TO HARD X-RAY OBSERVATIONS OF NEUTRON STAR BINARIES

Object	Time	Experiment(s)	Range (keV)	Model	Parameters	F_X (ergs cm^{-2} s^{-1})	F_{HX} (ergs cm^{-2} s^{-1})	References
4U 0614+09	1991 Aug–Sep	BATSE	20–200	PL	2.2	2.3×10^{-9}	1.1×10^{-9}	1, 2
Cen X-4	1979 May	*Ariel V* and SIGNE 2	12–160	CPL[a]	1.0, 45.0	5.7×10^{-8}	5.0×10^{-8}	3
4U 1608−52	1991 Jun–Dec	BATSE and *Ginga*	20–200	BPL	1.75, 3.2, 65.0	2.8×10^{-9}	2.9×10^{-9}	4
4U 1705−44	1993 Dec–1994 Jan	BATSE	20–200	BPL	1.5, 2.7, 70	1.3×10^{-9}	1.7×10^{-9}	5, 6
1E 1724−3045[b].....	1990 Mar–Apr	SIGMA	35–200	PL	1.7	5.6×10^{-10}	9.8×10^{-10}	7
GX 354−0	1992 Nov–Dec	BATSE	20–200	BPL	2.0, 3.0, 70.0	6.2×10^{-9}	3.9×10^{-9}	8, 9
KS 1731−260	1991 Mar 14	SIGMA	35–150	TB[c]	40.0	2.8×10^{-9}	2.4×10^{-9}	10
SLX 1732−304	1990 Mar–1994 Apr	SIGMA	35–150	BPL	2.0, 3.0, 70.0	2.4×10^{-10}	1.5×10^{-10}	11, 12
A 1742−294	1992 Sep and Oct	SIGMA	35–150	TB[c]	40.0	6.4×10^{-10}	5.5×10^{-10}	13
Aql X-1	1991 Aug–Sep	BATSE	20–200	PL[c]	2.6	1.4×10^{-8}	2.1×10^{-9}	14

NOTE.—Quasi-simultaneous observations exist only for Cen X-4 and 4U 1608−52. Range defines the energy range of the hard X-ray observations. The models (parameters) are the same as those defined in Table 4. In addition, CPL means cutoff power law. The parameters are α: photon index and E_{Cutoff} cutoff energy. F_X is the X-ray flux in the 1–20 keV band, whereas F_{HX} is the hard X-ray flux in the 20–200 keV band.

[a] Only a simultaneous flux in the 3–6 keV band is available. To estimate F_X we have assumed the spectral shape observed at hard X-ray energies.

[b] Observations corresponding to the hardest and brightest state ever observed for the source in the hard X-ray band (Barret et al. 1991).

[c] F_X is derived from an extrapolation of the best-fit hard X-ray spectral parameters.

REFERENCES.—(1) Ford et al. 1996; (2) Barret & Grindlay 1995 for X-ray observations; (3) Bouchacourt et al. 1984; (4) Zhang et al. 1996a; (5) Barret et al. 1996; (6) Langmeier et al. 1987 (for low state X-ray observations); (7) Barret et al. 1991; (8) Harmon et al. 1993a; (9) Barret & Grindlay 1996; (10) Barret et al. 1992a; (11) Goldwurm et al. 1995; (12) In't Zand 1992; (13) Churazov et al. 1995; (14) Harmon et al. 1996.

We estimated F_X and F_{HX}[6] from the *Ariel V* observation that took place between 1975 August 20 and 23, which is about one week after the peak of the outburst (Coe et al. 1976).

3. THE NEUTRON STAR BINARIES (NSBs)

There are only two NSBs for which quasi-simultaneous X-ray/hard X-ray observations exist, namely, 4U 1608−52 and Cen X-4.

4U 1608−52 underwent an outburst of 6 month duration in the hard X-ray band between 1991 June and December. This outburst was monitored by the *CGRO* BATSE experiment (Zhang et al. 1996a). In the middle of the outburst, *Ginga* observed 4U 1608−52 and found that the source was in a low X-ray state and that its X-ray spectrum had a power-law shape (Yoshida et al. 1993). These quasi-simultaneous observations showed for the first time that the hard X-ray emission from X-ray bursters was associated with a low X-ray intensity state, as had been anticipated (Barret & Vedrenne 1994; van Paradijs & van der Klis 1994). A combined fit of the *Ginga* and BATSE data indicates that the overall spectrum is best described by a broken power law with $\alpha_1 = 1.75$, $\alpha_2 = 3.2$ and a break at ~ 65 keV (Zhang et al. 1996a). This model has been assumed to compute F_X and F_{HX} given in Table 5.

The 1979 outburst of the soft X-ray transient Cen X-4 was observed simultaneously in X-rays by the *Ariel V* All Sky Monitor (Kaluzienski et al. 1980) and by *Hakucho* (Matsuoka et al. 1980), and in hard X-rays (13–163 keV) by SIGNE 2 MP (Bouchacourt et al. 1984). A comparison of the X-ray and hard X-ray light curves shows that the hard X-ray flux appeared first. Initially the hard flux rose rapidly, but it decreased and then disappeared by the time the X-ray flux had reached its maximum intensity. As with 4U

[6] The hard X-ray flux estimated from an extrapolation of the power-law tail in the *OSO 8* data (White et al. 1984) is within a factor of 2 of the value obtained using *Ariel V* data (Coe, Engel, & Quenby 1976).

1608−52, hard X-ray emission from Cen X-4 was associated with a low X-ray flux. The hard X-ray spectra recorded during the rise of the outburst can be fitted by a cutoff power law with a cutoff energy around 45 keV (Bouchacourt et al. 1984). Assuming this spectral shape and using a simultaneous determination of the *Ariel V*/ASM 3–6 keV photon flux ($\sim$1.4 photons cm^{-2} s^{-1}, Kaluzienski et al. 1980), we obtain the estimates for F_X and F_{HX} given in Table 5.

For the eight remaining sources, we have only F_{HX} and the shape of the hard X-ray spectrum; F_X has to be estimated separately. We first considered the sources that have displayed luminosity-related spectral changes similar to those observed for 4U 1608−52 and Cen X-4: 1E 1724−3045, SLX 1732−304, GX 354−0, 4U 1705−44, and 4U 0614+09.[7] At X-ray energies these sources display power-law spectra in their low intensity states. Consequently (based on the results for 4U 1608−52 and Cen X-4), we *assume* that the hard X-ray tail is associated with a low X-ray state, and the overall spectrum is a broken power law. The broken power-law model used in computing F_X was constructed as follows: α_1 (typically $\sim$2) was derived from the (nonsimultaneous) low state X-ray observations, whereas for α_2 (typically $\sim$3) we used the photon index of the hard X-ray tail. We fixed the break energy at 70 keV (the approximate value observed for 4U 1608−52 by Zhang et al. 1996a); finally we normalized F_X to match the observed hard X-ray flux. In two cases 1E 1724−3045 and 4U 0614+09, the observed values of α_1 and α_2 are comparable ($\sim$2), so we adopted a single power-law index, α_2 (i.e., no break).

The X-ray burster 1E 1724−3045 (in the globular cluster Terzan 2) is a source of persistent emission in the hard X-ray band; its 35–75 keV flux varies from 10 to 50 mCrab (Godwurm et al. 1995). The brightest state of the source in hard X-rays was observed by SIGMA on 1990 March-April (Barret et al. 1991). The source was then characterized by an unusually flat, hard X-ray spectrum ($\alpha \sim 1.7 \pm 0.5$, Barret et al. 1991). We have estimated F_X by simply extrapolating this power-law spectrum down to 1 keV. The source's hard X-ray flux averaged over 4 yr of observations is $\sim$20 mCrab (35–75 keV; Goldwurm et al. 1995). The time-averaged hard X-ray spectrum is steep ($\alpha \sim 3$) and similar to those observed for the other X-ray bursters detected by SIGMA. Consider the broken power law for a moment. Using the average value for F_{HX} ($\sim 4.4 \times 10^{-10}$ ergs cm^{-2} s^{-1}) and α_1 from TTM observations (In't Zand 1992), we find $F_X \sim 8.9 \times 10^{-10}$ ergs cm^{-2} s^{-1}. These fluxes are similar (within a factor of 2) to the fluxes associated with the brightest hard X-ray state (Table 5).

SLX 1732−304 (in the globular cluster Terzan 1) is a very weak source in the hard X-ray band with an averaged flux of $\sim$7.4 mCrab (35–75 keV; Goldwurm et al. 1995). Consequently, nothing is known about source variability. We used the averaged hard X-ray flux and the broken power law to compute F_X.[8] For this source, α_1 has been derived from TTM observations (In't Zand 1992).

GX 354−0 displays outburst-like events in the hard X-ray band and also maintains low-level persistent emission between outbursts (Claret et al. 1994; Harmon et al. 1993a; Goldwurm et al. 1995). The brightest hard X-ray outburst of this source was recorded by BATSE in 1992 November–December (Harmon et al. 1993a). Low-state X-ray observations are taken from Barret & Grindlay (1996).

The source 4U 1705−44 underwent a hard X-ray outburst in 1993 December–1994 January. BATSE monitored this outburst and detected the source for the first time at 100 keV (Barret et al. 1996). Low-state X-ray observations of this source have been reported by Langmeier et al. (1987).

The first detection of 4U 0614+09 at 100 keV was made by BATSE in 1991 September–October (Ford et al. 1996). The hard X-ray spectrum is best fitted by a power law of photon index $\sim$2.2 with no evidence for a break (or cutoff). Since the low-state X-ray spectrum is also a power law with index around 2.0 (Barret & Grindlay 1995; Singh & Apparao 1994), we have estimated F_X by extrapolating the BATSE spectrum.

There are three remaining NSBs for which no evidence for a low/hard state in X-rays exists, namely, Aql X-1, KS 1731−260, and A1742−294. The latter two sources are the most poorly studied of the NSBs considered here. SIGMA observed hard X-ray outbursts from A1742−294 in the fall of 1992 (Churazov et al. 1995) and from KS 1731−260 on 1991 March 14 (Barret et al. 1992a). For both sources, the overall shape of the hard X-ray spectrum was a steep ($\alpha \sim 3$) power law. It is probable that the spectrum is significantly flatter in the X-ray band. Therefore, to avoid a gross overestimate of the X-ray flux, we used a 40 keV thermal bremsstrahlung model[9] in extrapolating the hard X-ray spectrum down to 1 keV.

Several hard X-ray outbursts have been observed from the X-ray transient Aql X-1 by BATSE between 1991 and 1994 (Harmon et al. 1996). One of the brightest was recorded in 1991 during the period August 22–September 1. The 20–200 keV spectrum was a steep power law of index 2.6, and there was no evidence for a break or cutoff. This photon index is significantly larger than the values of α_1 observed for X-ray bursters in their X-ray low states. Nevertheless, we used this index to extrapolate the hard X-ray spectrum down to 1 keV, which means that we have probably somewhat overestimated F_X for Aql X-1. We note that our estimates for F_X are relatively uncertain for those sources that lack simultaneous X-ray data because the flux depends strongly on the spectral shape assumed in X-rays. Furthermore, the fact that the ratio F_X/F_{HX} is close to unity for most of these sources (see Table 5) is a consequence of the assumptions we made in estimating their X-ray to hard X-ray spectra (see above).

4. THE BLACK HOLE CANDIDATES (BHCs)

Table 6 lists the observations of BHCs that we use in this paper. Only five BHCs have simultaneous or quasi-simultaneous X-ray and hard X-ray observations, namely, GX 339−4 in its low X-ray state (*Granat*, Grebenev et al. 1993), 1E 1740.7−2942 (*Granat*, Grebenev et al. 1995), GRS 1009−45 (*Kvant*; Sunyaev et al. 1994), GRS 1716−249

[7] Note that GX 354−0, 4U 1705−44, and 4U 0614+09 are all "Atoll" sources that share timing similarities with 4U 1608−52, also a well-known "Atoll" source (Hasinger & van der Klis 1989).

[8] See Pavlinsky et al. (1995) for a comparison of the X-ray and hard X-ray observations showing that the hard X-ray emission is likely to be associated with a low X-ray state.

[9] The thermal bremsstrahlung model resembles the cutoff power law model and is therefore likely to provide a more realistic description of the X-ray/hard X-ray spectrum than the steep power law. Note also that the thermal bremsstrahlung model and the power-law model fit the data equally well (e.g., A1742−294; Churazov et al. 1995).

TABLE 6

BLACK HOLE CANDIDATES

Object	Time	Experiments	Range (keV)	US[a] (Y/N)	Model	Parameters	F_X (ergs cm^{-2} s^{-1})	F_{HX} (ergs cm^{-2} s^{-1})	References
GRO J0422+32.....	1992 Aug 29	*Kvant*	2–300	N	S&T	28.0, 2.00	1.8×10^{-8}	3.9×10^{-8}	1
LMC X-1	1989 Nov 13–Dec 2	TTM	2–30	Y	D + PL[b]	39.0(50), 0.83	6.7×10^{-10}	2.8×10^{-11}	2
GRS 1009−45.....	1993 Sep 30	*Kvant*	1–200	Y	B + PL[b]	0.5, 2.5	2.2×10^{-8}	1.1×10^{-9}	3
GS 1354−64.....	1987 Feb–Apr	*Ginga*	1–10	Y	D + PL[b]	51.0(10), 0.7, 2.1	1.0×10^{-8}	1.3×10^{-9}	4
A1524−62	1990 Aug 27	SIGMA	35–100	?	PL[c]	1.8	1.5×10^{-9}	2.0×10^{-9}	5
4U 1543−47.....	1992 Apr 19–25	BATSE	20–200	?	PL[c]	2.7	8.4×10^{-8}	1.2×10^{-8}	6
4U 1630−47.....	1984 Apr 11	*EXOSAT*	1–20	Y	CPL + PL[b]	1.8, 1.15, 2.48	2.2×10^{-8}	2.4×10^{-9}	7
GX 339−4[d].....	1988 Sep 4	*Ginga*	1–30	Y	D + PL[b]	15.2(4), 0.9, 2.7	3.2×10^{-8}	1.8×10^{-9}	8
GX 339−4.....	1983 May 14	*Tenma*	1–20	Y	D + PL[b]	20.5(4), 0.8, 2.1	1.4×10^{-8}	6.8×10^{-10}	9
GX 339−4.....	1990 Aug 18	ART-P	3–20	Y	D[e]	16.4(4), 0.8	8.7×10^{-9}	$<1.2 \times 10^{-10}$	10
GX 339−4.....	1990 Mar–Apr	*Granat*	1–200	N	S&T	30.0, 1.65	2.4×10^{-9}	3.8×10^{-9}	10
GRS 1716−249	1992 Oct	*Kvant*	1–200	N	TB	117.0	1.3×10^{-8}	2.9×10^{-8}	11
KS 1730−312	1994 Sep 26	TTM	2–27	N	PL	2.7	2.2×10^{-8}	2.5×10^{-9}	12
1E 1740.7−2942.....	1996 Mar–Apr	*Granat*	4–400	N	S&T	35, 1.5	1.9×10^{-9}	2.6×10^{-9}	13
H1743−322.....	1977 Aug	*HEAO 1*	10–200	Y	TB + PL[f]	1.0, 2.4	2.6×10^{-8}	2.7×10^{-9}	14
X1755−338	1989 Sep 10	TTM	2–30	Y	D + PL[b]	5.1(9), 1.28, 2.3	3.0×10^{-9}	5.1×10^{-10}	2
GRS 1758−258	1990 Sep–Oct	SIGMA	35–300	N	S&T[e]	38, 1.12	2.1×10^{-9}	2.0×10^{-9}	15
GS 1826−24.....	1992 Dec 15–31	*OSSE*	50–200	N	CPL[b,g]	1.7, 60	9.5×10^{-10}	7.0×10^{-10}	16
EXO 1846−031	1984 Apr 3–4	*EXOSAT*	1–20	Y	D + PL[b]	21.6(7), 0.96, 2.6	1.9×10^{-8}	8.5×10^{-10}	17
GRS 1915+105	1992 Sep 23–24	*Granat*	1–200	N	PL[c]	2.5	1.7×10^{-8}	3.4×10^{-9}	18
4U 1957+11.....	1990 Sep 24	*Ginga*	1–18	Y	D + PL[b]	1.7(7), 1.56, 2.12	1.2×10^{-9}	3.0×10^{-10}	19

NOTE.—X-ray (1–20 keV) and hard X-ray observations of black hole candidates (BHCs). "Range" defines the energy range of the observations. The models (parameters) are the same as those defined in Tables 4 and 5. F_X is the X-ray flux in the 1–20 keV band, whereas F_{HX} is the hard X-ray flux in the 20–200 keV band.

[a] Indicates the presence of an ultrasoft component in the spectrum.

[b] F_{HX} is extrapolated from the power-law tail observed in X-rays.

[c] F_X is derived from an extrapolation to X-rays of the best-fit hard X-ray spectral parameters.

[d] The four observations correspond to four different spectral states, ordered by decreasing X-ray flux: very high state (ultrasoft component and power-law tail), high state (ultrasoft component and power-law tail), high state (ultrasoft component without power tail), and low state (no ultrasoft component). The upper limit on F_{HX} is derived from the ART-P observation (assuming a power law photon index of 2).

[e] R_{max} and T_{max} are derived from a fit by the original Shakura-Sunyaev (1973) disk blackbody model.

[f] H1743−22 displayed an ultrasoft component for which we have assumed a 1 keV bremsstrahlung for the spectral shape (no spectral parameters have ever been published). This component was normalized to the maximum X-ray flux given in Tanaka & Lewin (1995).

[g] The spectral shape was determined from a comparison of non simultaneous *Ginga* and *OSSE* data (see Strickman et al. 1996b for details).

REFERENCES.—(1) Sunyaev et al. 1993b; (2) Pan et al. 1995; (3) Sunyaev et al. 1994; (4) Kitamoto et al. 1990; (5) Barret et al. 1992b; (6) Harmon et al. 1993b; (7) Parmar et al. 1986; (8) Miyamoto et al. 1991; (9) Makishima et al. 1986; (10) Grebenev et al. 1991; (11) Grebenev et al. 1993; (12) Borozdin et al. 1995; (13) Grebenev et al. 1995; (14) Cooke et al. 1984; (15) Gilfanov et al. 1993b; (16) Strickman et al. 1996b; (17) Parmar et al. 1993; (18) Sazonov et al. 1994; (19) Yaqoob et al. 1993.

(*Kvant*, Sunyaev et al. 1994) and GRS 1915+105 (*Granat*, Sazonov et al. 1994). About a dozen additional sources have been observed only up to ~20–30 keV by missions such as *Tenma*, EXOSAT, *Ginga*, and TTM. These sources display a hard tail with a power-law shape (e.g., LMC X-1, 4U 1630−47, X1755−338, 4U 1957+11, etc.). Broadband observations of BHBs have shown that such power-law tails can be extrapolated successfully in the hard X-ray band (e.g., Grebenev et al. 1993). Therefore to estimate the hard X-ray flux, we have simply extrapolated the X-ray power law up to 200 keV. We have assumed that there is no break or cutoff in the hard X-ray spectrum. We have checked that for the typical photon index observed (i.e., between 2.0 and 2.7), if a cutoff were present at 150 keV, for example, this would lead us to overestimate F_{HX} by less than a factor of 2. Similarly, we have examined the sensitivity of our results to uncertainties in the power-law index (see Tanaka & Lewin 1995). For the same normalization flux at 30 keV (which is the high-energy threshold of the experiments listed above), a power law of index 1.5 yields a 20–200 keV flux about twice larger than the flux corresponding to a power law of index 2.5. Again, a simple extrapolation is not likely to affect our results significantly.

Finally, for the remaining sources we compute F_X by extrapolating the hard X-ray best-fit spectrum down to the X-ray band. In the case of GRS 1758−258, for example, nonsimultaneous X-ray observations (Gilfanov et al. 1993b) have shown that the observed X-ray spectrum is consistent with such an extrapolation.

For GX 339−4, a particularly well-known BHC, we have considered four observations corresponding to four different spectral states in X-rays (a very high state, two high states, and a low state, respectively; Tanaka & Lewin 1995). It is obvious that some of the BBCs have been observed several times with different experiments, and very likely at different intensity levels. Although we have surveyed the literature extensively, it remains possible that some of the values of F_{HX} listed in Table 6 are not the absolute maximum values.

5. DISCUSSION

In the following, we compare first the BHBs with the NSBs, and then the BHCs with the NSBs.

5.1. *BHBs versus NSBs*

In Figure 1 we plot the hard X-ray luminosities versus the X-ray luminosities of BHBs and NSBs. A striking feature of the figure is that *when both BHBs and NSBs emit hard X-rays, only BHBs seem to emit hard X-ray tails associated with a simultaneous X-ray luminosity larger than* $\sim 1 \times 10^{37}$ *ergs* s^{-1} *and/or have hard X-ray tails with* L_{HX} *larger than* $\sim 1 \times 10^{37}$ *ergs* s^{-1}. None of the NSBs exceeds a total luminosity of $\sim 2 \times 10^{37}$ ergs s^{-1} when a hard tail is in evidence. This is relatively low, only about $0.1 \times L_{Edd}$ for a 1.4 $M_\odot$ neutron star ($L_{Edd} = 1.3 \times 10^{38} M_{NS}/M_\odot$ ergs s^{-1}). Note that NSBs can reach much greater luminosities in their high X-ray states, but their hard X-ray luminosities are then very low (e.g., 4U 1608−52, see below).

In Figure 1 we have drawn arbitrarily a retangular box, called the "X-ray burster box," with boundaries defined by the maximum L_X and L_{HX} observed from NSBs (i.e., $\sim 1.5 \times 10^{37}$ ergs s^{-1} and $\sim 1.3 \times 10^{37}$ ergs s^{-1}, respectively) when they emit hard X-ray tails. For simplicity we have chosen to draw a box although no sources are

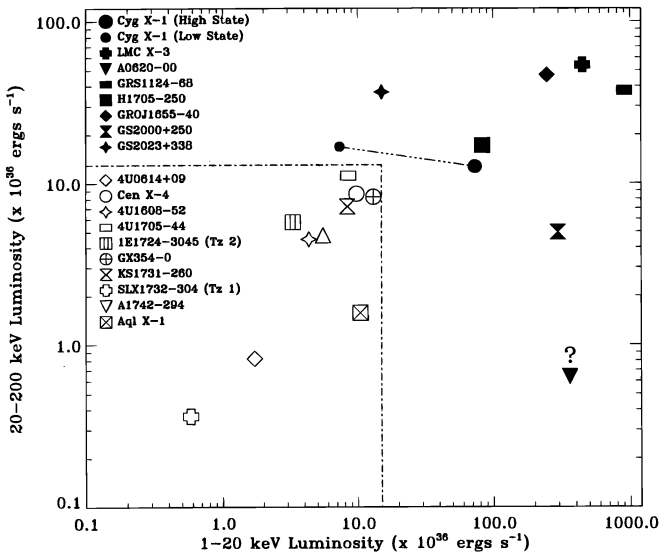

FIG. 1.—Hard X-ray vs. X-ray luminosities of BHBs and NSBs. Filled symbols are for BHBs and open symbols for NSBs. The dot-dashed line defines the X-ray burster box.

expected to be found in the region where L_{HX} is much larger than L_X (this would require unplausibly hard spectra not observed from any kind of X-ray binary including BHBs and BHCs). We note that a vertical line at $L_X \sim 10^{37}$ ergs s^{-1} could also be used to separate the BHBs from the NSBs as suggested by Barret & Vedrenne (1994) and van Paradijs & van der Klis (1994).

In Figure 1, two classes of BHBs can be distinguished. The first class contains those systems displaying an ultrasoft component. They have $L_X \gtrsim 10^{38}$ ergs s^{-1}. The five ultrasoft X-ray transients (i.e., excluding GS 2023+338) have an average X-ray luminosity of 3.8×10^{38} ergs s^{-1}. For these sources, less than ~20% of the total luminosity is radiated in hard X-rays; for GS 2000+250 it is only about 2%.

The second class of sources includes Cyg X-1 (low state) and GS 2023+338, systems which do not show such an ultrasoft component. Unlike the ultrasoft transients, they have L_{HX} larger than L_X due to their hard spectra ($\alpha \sim 1.5$–1.7) and are located relatively close to the X-ray burster box. In the figure, we show the location of Cyg X-1 in its high state based on the spectral parameters given in Oda (1977).[10] In going from the low to the high state, Cyg X-1 switches from a hard power-law spectrum to an ultrasoft spectrum in X-rays.

As shown in Figure 1, NSBs have L_X comparable to L_{HX}. This may also be a noticeable difference between NSBs and BHBs (at least those BHBs with ultrasoft components). We note that the line for which $L_X = L_{HX}$ corresponds to a power law of photon index ~1.9.

As mentioned in § 2, the X-ray and hard X-ray luminosities used for the transient BHBs were not the peak values nor were they determined during the same point in the outburst cycle; therefore they are not directly comparable. Nevertheless, we searched for possible correlations

[10] According to Oda (1977), the X-ray to hard X-ray spectrum associated with the high state can be approximated by the sum of a steep power law $300 \times E_{keV}^{-5}$ and a hard power law $1.5 \times E_{keV}^{-1.6}$ photons cm^{-2} keV^{-1}. We use these parameters to compute F_X and F_{HX} associated with the high state of Cyg X-1.

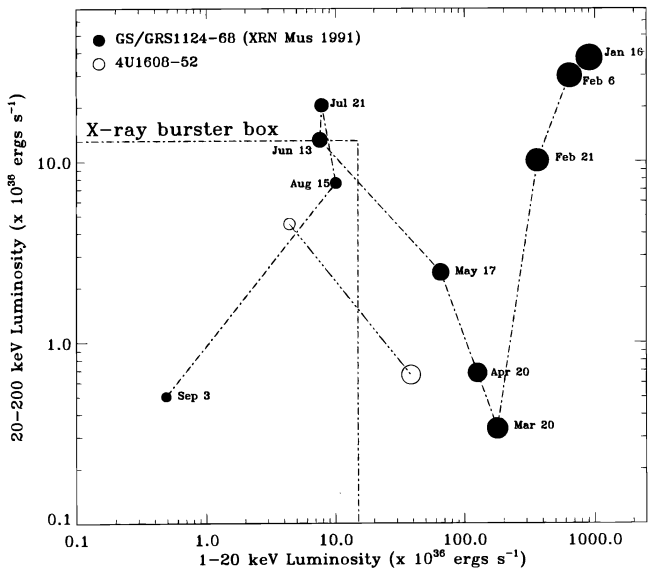

FIG. 2.—Evolution of L_X and L_{HX} for GRS 1124−68 after its X-ray maximum, which occurred on 1991 January 15. The outburst started on January 8. From the top right to the bottom left of the plot the observation times are (1991): January 16 (*Ginga* and SIGMA), February 6 (*Ginga* and SIGMA), February 21 (*Ginga*), March 20 (*Ginga*), April 19 (*Ginga*), May 17 (*Ginga*), June 13 (*Ginga*), July 21 (*Ginga*), August 15 (ART-P and SIGMA). September 3 (*Ginga*, last detection). The size of each point (*filled circle*) is plotted as proportional to the L_X value at that point of the outburst. For the *Ginga* observations alone, the hard X-ray flux has been extrapolated from the observed power-law tail. References are Ebisawa et al. (1994) for *Ginga* data, Goldwurm et al. (1992) for SIGMA data, and Grebenev et al. (1992) for ART-P data. The positions of the X-ray burster 4U 1608−52 (*open circle*) in its high and low X-ray states are also shown for comparison. Data are taken from Mitsuda et al. (1989) and Zhang et al. (1996a), respectively.

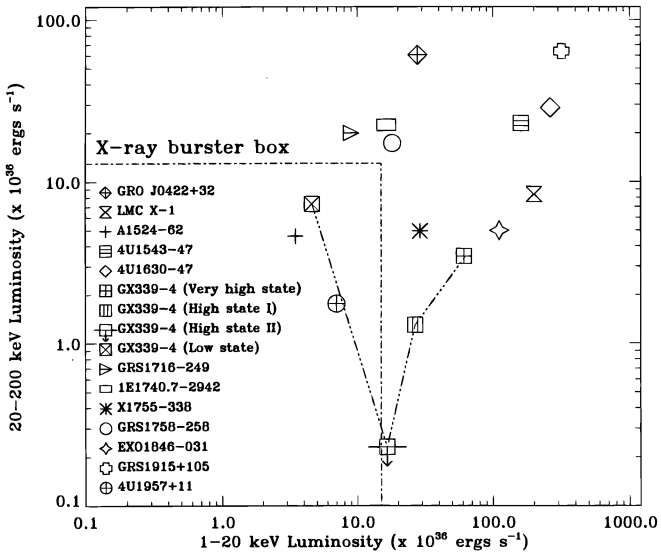

FIG. 3.—Hard X-ray vs. X-ray luminosities of BHCs and NSBs. The X-ray burster box is defined in Fig. 1.

between the mass of the compact object and L_X, L_{HX}, and L_{Total}. No such correlations were found.

As an illustration of the spectral variability of BH X-ray transients, in Figure 2 we show the trajectory of GRS 1124−68 in the L_X-L_{HX} plane as it decayed in intensity following its 1991 outburst (Ebisawa et al. 1994; Goldwurm et al. 1992; Grebenev et al. 1992). Early in the outburst cycle, most of the energy was radiated in the ultrasoft component, and the hard X-ray component was unimportant. As the nova decayed, the hard X-ray luminosity decayed rapidly and became very faint in March–April (i.e., about 70 days after the initial outburst). For a few months around this time, L_{HX} was then in the range observed for NSBs, although the X-ray luminosity was considerably greater than the luminosities of NSBs. After reaching a minimum, the hard X-ray luminosity began to increase while the X-ray luminosity continued to decrease. Later in the outburst, GRS 1124−68 spent some time in the X-ray burster box. At still later times, both the X-ray and hard X-ray luminosities further decreased as the source returned to quiescence. In quiescence the X-ray luminosity is very low: $L_X \leq 2.2 \times 10^{32}$ ergs s^{-1} (Greiner et al. 1994).

Figure 2 illustrates that the high luminosity in hard X-rays distinguishes GRS 1124−68 from NSBs only during the first several weeks of the outburst. Note also that during this period, L_X was larger than L_{Edd} for a NS. As the *X*-ray luminosity approached $\sim 10^{38}$ ergs s^{-1} (March–April), the source's location in the L_X/L_{HX} diagram moved toward the position where one expects to find the NSBs in their high X-ray states (i.e., with $L_X \sim 5 \times 10^{37}$–$1 \times 10^{38}$ ergs s^{-1}, e.g., 4U 1608−52, see below) including the bright *Z*-sources (e.g., Sco X-1; Hasinger & van der Klis 1989). A distinction, however, is that NS sources do not appear to display hard power-law tails.[11] At still later stages in the outburst for which L_X or $L_{HX} \lesssim 10^{37}$ ergs s^{-1}, GRS 1124−68 resembles the NSBs.

In Figure 2 we also show the trajectory of the X-ray burster 4U 1608−52 as it evolves from its high (also called "banana") to its low (or "island") X-ray state (i.e., from the right to the left in the L_X–L_{HX} diagram). The high state data are from Mitsuda et al. (1989) and the low state data are from Zhang et al. (1996a). In the high state, the X-ray spectrum has a thermal shape and there is no detectable hard tail (up to the upper end of the *Tenma* energy range ~ 30 keV). L_{HX} is estimated from the extrapolation of the X-ray spectrum (and not from the presence of a detected hard tail) and is significantly lower than L_X. In its high state, 4U 1608−52 falls outside the X-ray burster box and is located in the region of the L_X–L_{HX} plane where one expects to find the X-ray bright NS systems. In the low state, the X-ray spectrum has a power-law shape which extrapolates to a hard tail with L_{HX} comparable to L_X (Zhang et al. 1996a). The slope of the trajectory of 4U 1608−52 in Figure 2 (though determined by only two points) is similar to that of Nova Muscae as it evolved from mid-outburst to the end of its outburst. (This hardness-intensity behavior is often referred to as the X-ray/hard X-ray anticorrelation; see, for example Tanaka 1989). This slope is significantly steeper than the trajectory of Cyg X-1 in its transition from the high to the low state (see Fig. 1).

5.2. *BHCs versus NSBs*

In Figure 3 we compare the luminosities of the BHCs for which distance estimates exist and the NSBs, which are represented by the X-ray burster box. One can divide the BHCs plotted in the figure in three groups. The first group contains the most X-ray luminous BHCs: GRS 1915+105,

[11] There may be, however, evidence for a weak and steep hard tail in Sco X-1 according to recent *CGRO* OSSE observations (Strickman et al. 1996a).

LMC X-1, 4U 1630−47, and 4U 1543−47. These sources are located significantly outside the X-ray burster box, thus supporting the idea that they may be powered by accretion onto black holes. Their total luminosity is often well above the Eddington limit for a neutron star ($L_{\rm Edd}$). GRS 1915+105 is the most luminous source in X-rays among the BHCs. This is partially due to its rather steep X-ray/hard X-ray power-law spectrum ($\alpha = 2.5$, Sazonov et al. 1994). It is probable that LMC X-1 contains a black hole if, as seems likely, the optical counterpart is a $\sim 20\ M_\odot$ O star (Hutchings et al. 1987).

There is a second, distinctive group of sources in Figure 3 which lie just above the top right corner of the X-ray burster box with $L_X \sim 10^{37}$ ergs s^{-1} and $L_{\rm HX} \sim 2 \times 10^{37}$ ergs s^{-1}. This group is comprised of GRO J0422+32, 1E 1740.7−2942, GRS J1716−249, and GRS 1758−258. None of these BHCs displays an ultrasoft component. They lie near the positions of Cyg X-1 (low state) and GS 2023+338 (see Fig. 1), which suggests that they may contain a BH. They have $L_{\rm HX}$ larger than L_X due to their flat power-law spectra (photon index $\sim$1.6–1.7 and energy cutoff above 100 keV). We note that GRO J0422+32 probably contains a BH despite its low mass function ($f[M] = 1.21 \pm 0.06\ M_\odot$; Filippenko, Matheson & Ho 1995b).

The third group of sources is those defined by low $L_{\rm HX}$, namely, A1524−62, X1755−338, EXO 1846−031, and 4U 1957+11. The position of A1524−62 (Tra X-1) may be misleading because the hard X-ray observation was made during a low-intensity outburst in 1990 rather than during the more intense outburst in 1975 (Barret et al. 1995a). Also, if the source spectrum in 1990 had an ultrasoft component (as it did in 1975), we will have underestimated F_X, which we computed by simply extrapolating the hard X-ray power law to low energies (Barret et al. 1992b). X1755−338 and EXO 1846−031, which are both characterized by a bright ultrasoft component and a power-law tail, fall outside the X-ray burster box. Although the hard X-ray luminosity of EXO 1846−031 is in the range observed for NSBs, its large X-ray luminosity ($\sim 10^{38}$ ergs s^{-1}) suggests that the primary may be a BH.[12] A similar but weaker conclusion can be drawn for X1755−338 whose X-ray luminosity is only a factor of 2 greater than the limiting X-ray luminosity defined by the X-ray burster box.

The source 4U 1957+11 is puzzling. It was proposed as a BHC because of its ultrasoft X-ray spectrum and power-law tail. However, Yaqoob, Ebisawa, & Mitsuda (1994), using *Ginga* data fitted the ultrasoft component with a multicolor blackbody model (Mitsuda et al. 1984) and derived a projected inner radius ($R_{\rm in}\sqrt{\cos i}$) of $\sim$2 km (at 7 kpc), which is significantly smaller than the values observed for BHBs (typically 30–40 km; Tanaka & Lewin 1995). Due to the low amplitude of the modulation of its optical light curve, 4U 1957+11 is thought to be a low inclination system (van Paradijs & McClintock 1995). Therefore the projected radius should not differ significantly from the actual radius ($R_{\rm in}$). Furthermore, the inner disk temperature derived from the same fit is consistent with the values observed for other NS systems (e.g., 4U 1608−52 in its high state). Yaqoob et al. (1994) tentatively concluded that 4U 1957+11 contains a neutron star (see also Singh, Apparao, & Kraft 1994). Our result, which is based on the low X-ray and hard X-ray luminosities of the source, provides some additional support for the NS hypothesis.[13] If it turns out that 4U 1957+11 contains a NS, this would imply that a spectrum composed of an ultrasoft component and a power-law tail is not a unique signature of a BH, as has been suggested (White 1993).

Finally, the case of GX 339−4 is especially interesting because it is a leading BHC that exhibits several distinct X-ray spectral states similar to those observed from BHBs, in particular very high, high, and low states (Tanaka & Lewin 1995). However, it was discussed as a possible NS system following the report of a 1.13 ms optical period (Imamura et al. 1987), a result that has not been confirmed. The distance to the source is quite uncertain; the value of 4 kpc (Cowley, Crampton, & Hutchings 1987) that we have adopted is the distance most often used in the literature (e.g., Tanaka & Lewin 1995). In its low state, which is associated with the largest hard X-ray flux, GX 339−4 is located inside the X-ray burster box (see Fig. 3). On the other hand, GX 339−4 falls outside the X-ray burster box when it is in any of its "high" states. However, a recent study of the scattering halo around the source by *ROSAT* indicates that GX 339−4 may be as close as 1.3 kpc (Predehl et al. 1991), in full agreement with a similar study done by Mauche & Gorenstein (1986) using *Einstein* IPC data. This would reduce the luminosities by a factor of 10 and move the source well inside the X-ray burster box for all four of its spectral states (Fig. 3). Furthermore, at a distance of only 1.3 kpc, the inner disk radius derived from the fit of the ultrasoft component, which is present in the very high state and in the high states of the source, would become comparable to the values observed for NSBs (Miyamoto et al. 1991).

On the other hand, we note that the trajectory of GX 339−4 in the L_X–$L_{\rm HX}$ plane as it evolves from its very high X-ray state to its low X-ray state (thereby tracing out a "V" from right to left in Fig. 3) is similar to the trajectory shown for GRS 1124−68 as it decayed in intensity following its outburst (see Fig. 2). This similarity and the fact that GX 339−4 emits a hard X-ray tail in its very high X-ray state (which has not been observed for any confirmed NS systems) argues in favor of a BH primary in GX 339−4. This would argue, in turn, for the 4 kpc distance. Given the distance uncertainty, however, we cannot reach a firm conclusion.

For the five remaining BHCs, which do not have distance estimates listed in Table 3, we have computed their luminosities assuming their distances to be in the range 5–10 kpc. This range contains the average distance ($\sim$6.7 kpc) of the 12 BHCs that do have distances listed in Table 3. The lower bound of 5 kpc seems plausible given the 3.9 kpc average distance of the bright and well-studied BHBs (see above). The luminosities of these five objects are shown in Figure 4. Even at 5 kpc the luminosities of GRS 1009−45, GS 1354−64, KS 1730−312, and H1743−322 fall outside the X-ray burster box, thus supporting the idea that these systems may contain BH primaries. On the other hand, the

[12] We note that this source might be confused with GRO J1849−03 discovered in the BATSE survey for faint transients (Grindlay et al. 1996; Zhang et al. 1996b).

[13] It is worth stressing that 4U 1957+11 was observed by *Ginga* during a relatively high state since the X-ray flux derived from the best fit is comparable to the value given in van Paradijs (1995) and larger than the average flux observed by Vela 5B over its 10 year monitoring of the source (Smale & Lochner 1992).

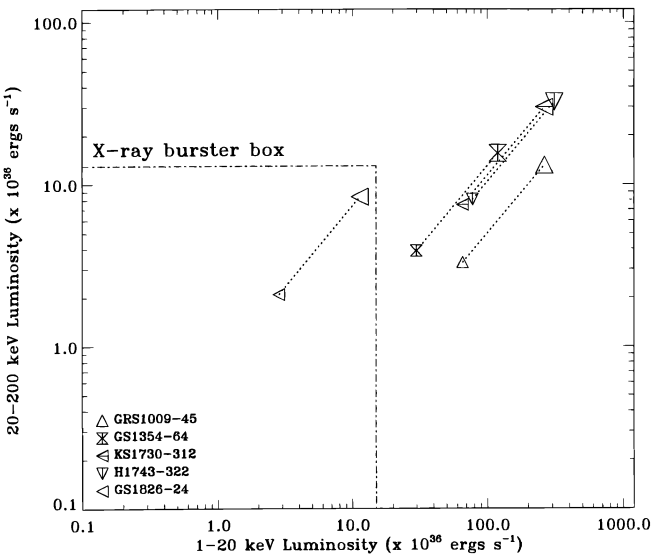

FIG. 4.—Hard X-ray vs. X-ray luminosities of BHCs with no distance estimates. For them we have assumed a plausible range of distances varying from 5 (*small symbol*) to 10 (*large symbol*) kpc. The X-ray burster box is defined in Fig. 1.

puzzling low-luminosity source GS 1826−24 (Tanaka 1989) is contained inside the X-ray burster box, even at a distance of 10 kpc. It is interesting to note that GS 1826−24 was recently discussed as a possible NS system because of its location inside the error box of an unknown burst source (van Paradijs 1995), and also because its timing/spectral X-ray/hard X-ray properties are very similar to those of low-luminosity X-ray bursters (Barret et al. 1995b; Strickman et al. 1996b).

To conclude, by comparing the X-ray and hard X-ray luminosities of BHCs and NSBs we have found that the five excellent BHCs—LMC X-1, GRO J0422+32, GRS 1915+105, 4U 1630−47, and 4U 1543−47—are clearly separated from the NSBs. We note that there is some dynamical evidence for BH primaries in the first two systems: LMC X-1 (Hutchings et al. 1987) and GRO J0422+32 (Filippenko, et al. 1995b). We have also found that 4U 1957+11 and GS 1826−24, two systems that have been previously referred to as possible NS systems, have positions in the L_X/L_{HX} diagram inside the X-ray burster box. Finally, GX 339−4 remains very problematic due to the large uncertainties in its distance estimate (from 1.3 to 4 kpc). At 1.3 kpc, even in its very high state, the X-ray and hard X-ray luminosities of the source would be consistent with those observed for NSBs. On the other hand, at 4 kpc, the position and the trajectory of the source in the L_X/L_{HX} diagram (see Fig. 3) make it plausible that GX 339−4 contains a BH.

We note that if either 4U 1957+11 or GX 339−4 is shown to be a BHB (and the distance to GX 339−4 is actually 1.3 kpc), then this would undermine the luminosity criteria proposed in this paper.

6. CONCLUSIONS

We conclude that the hard X-ray (20–200 keV) and X-ray (2–20 keV) luminosities can be used to distinguish BHBs from NSBs in several ways. First, although the presence of a hard X-ray tail is not a unique signature of BH accretion, the high luminosity in the hard tail does appear to be such a signature: only BHBs are observed to emit hard tails with $L_{HX} \gtrsim L_c$, where we define $L_c \sim 10^{37}$ ergs s^{-1} to be the critical luminosity. Second, the hard X-ray luminosities of NSBs can approach L_c, but only when $L_X \lesssim L_c$. On the other hand, BHBs can have both X-ray and hard X-ray luminosities above L_c (although the hard X-ray luminosity may be substantially below L_c). Third, a transient BHB may be found in the X-ray burster box ($L_X \lesssim L_c$ and $L_{HX} \lesssim L_c$) after its intensity has decayed significantly from maximum. Thus BHBs are distinguished from NSBs only at relatively high luminosities.

D. B. is grateful to Centre National d'Etudes Spatiales (CNES) for the support of a post-doctoral fellowship. This work was supported in part by NASA grant NAG5-2763. Additional support was also provided to J.E.M by the Smithsonian Institution Scholarly Studies Program. This research has made use of data obtained through the High Energy Astrophysics Science Archive Research Center Online Service, provided by the NASA/Goddard Space Flight Center. We are grateful to K. Ebisawa, A. Harmon, S. Grebenev, G. Vedrenne, S. Myamoto, N. White, and S. N. Zhang for discussions about some of the observations used in this paper, and H. Tananbaum and S. Grebenev for comments on the paper.

The authors wish to thank the referee J. van Paradijs for his helpful and insightful comments on the paper.

REFERENCES

Barret, D., et al. 1991, ApJ, 379, L21
———. 1992a, ApJ, 394, 615
———. 1992b, ApJ, 392, L19
———. 1995a, A&A, 296, 459
———. 1995b, A&A, 303, 526
———. 1996, A&AS, in press
Barret, D., & Grindlay, 1995, ApJ, 440, 841
———. 1996, A&A, in preparation
Barret, D., & Vedrenne, G. 1994, ApJS, 92, 505
Bailyn, C. D., Orosz, J. A., McClintock, J. E., & Remillard, R. A. 1995, Nature, 378, 157
Borozdin, K. N., et al. 1995, Soviet Astron. Lett., 21 (2), 212
Bouchacourt, P., Chambon, G., Niel, M., Refloch, A., Estulin, I. V., Kuznetsov, A. V., & Melioranskii, A. X. 1984, ApJ, 285, L67
Brandt, S., Castro-Tirado, A. J., Lund, N., Dremin, V., Lapshov, I., & Sunyaev, R. A. 1993, A&AS, 97, 257
Casares, J., Charles, P. A., & Marsh, T. R. 1995a, MNRAS, 277, L45
Casares, J., Martin, A. C., Charles, P. A., Martin, E. L., Rebolo, R., Harlaftis, E. T., & Castro-Tirado, A. J. 1995b, MNRAS, 276, L35
Chaty, S., Mirabel, I. F., Dac, P. A., Wink, J. E., & Rodriquez, L. F. 1996, A&A, 310, 825
Chevalier, C. 1989, in Proc. 23rd ESLAB Symp. (Bologna), ed. J. Hunt & B. Battrick (ESA SP-296), 341
Chevalier, C., Ilovaisky, S. A., van Paradijs, J., Pedersen, H., & van der Klis, M. 1989, A&A, 210, 114
Churazov, E., et al. 1995, ApJ, 443, 341
Claret, A., et al. 1994, ApJ, 423, 436
Coe, M. J., Engel, A. R., & Quenby, J. J. 1976, Nature, 256, 544
Cooke, B. A., Levine, A. M., Lang, F. L., Primini, F. A., & Lewin, W. H. G. 1984, ApJ, 285, 258
Cowley, A. P., Crampton, D., Hutchings, J. B., Remillard, R., & Penfold, J. E. 1983, ApJ, 272, 118
Cowley, A. P., Crampton, D., & Hutchings, J. B. 1987, AJ, 93, 195
Crary, D. J., et al. 1996, ApJ, 462, L71
Della Valle, M., Mirabel, I. F., & Rodriguez, L. F. 1994, A&A, 290, 803
Ebisawa, K., et al. 1994, PASJ, 46, 375
Filippenko, A. V., Matheson, T., & Barth, A. J. 1995a, ApJ, 455, L139
Filippenko, A. V., Matheson, T., & Ho, L. C. 1995b, ApJ, 455, 614
Frank, J., King, A. R. & Raine, D. J. 1992, in Accretion Power in Astrophysics (Cambridge: Cambridge Univ. Press), 51
Ford, E., et al. 1996, in preparation
Gies D. R., & Bolton, C. T. 1982, ApJ, 260, 240

Gies D. R., & Bolton, C. T. 1986, ApJ, 304, 371
Gilfanov, M., et al. 1993a, in The Lives of Neutron Stars, ed. M. A. Alpar, U. Kizilogu, & J. van Paradijs (Dordrecht: Kluwer), 331
———. 1993b, ApJ, 418, 844
Goldwurm, A., et al. 1992, ApJ, 389, L79
———. 1995, Adv. Space Res., 15, 41
Grebenev, S. A., et al. 1993, A&A, 97, 281
Grebenev, S. A., Pavlinsky, M. N., & Sunyaev, R. A. 1995, Adv. Space Res., 15, 115
Grebenev, S. A., Sunyaev, R. A., & Pavlinski, M. N. 1992, Soviet Astron. Lett., 18, 11
Grebenev, S. A., Sunyaev, R. A., Pavlinski, M. N., & Dekhanov, I. A. 1991, Soviet Astron. Lett., 17, 985
Greiner, J., Hasinger, G., Molendi, S., & Ebisawa, K. 1994, A&A, 285, 509
Grindlay, J. E. 1978, ApJ, 224, L107
Grindlay, J. E., et al. 1996, A&AS, in press
Haberl, F., & Titarchuk, L. 1995, A&A, 299, 414
Harmon, B. A., et al. 1993a, in AIP Conf. Proc. 304, 2nd Compton Symp., ed. C. E. Fichtel, N. Gehrels, & J. P. Norris (New York: AIP), 456
———. 1993b, in AIP Conf. Proc. 304, ed. C. E. Fichtel, N. Gehrels, & J. P. Norris (New York: AIP), 210
———. 1996, A&AS, in press
Hasinger, G., & van der Klis, M. 1989, A&A, 225, 79
Haswell, C. A., Robinson, E. L., Horne, K., Stiening, R., & Abbott, T. M. C. 1993, ApJ, 411, 802
Herrero, A., Kudritzki, R. P., Gabler, R., Vilchez, J. M., & Gabler, A. 1995, A&A, 297, 556
Hjellming, R. M., & Rupen, M. P. 1995, Nature, 375, 464
Hutchings, J. B., Crampton, D., Cowley, A. P., Bianchi, L., & Thompson, I. B. 1987, AJ, 94, 390
Imamura, J. N., Steiman-Cameron, T. Y., & Middleditch, J. 1987, ApJ, 314, L11
In't Zand, J. J. M. 1992, Ph.D. thesis, Univ. Utrecht
Kaluzienski, L. J., Holt, S. S., & Swank, J. H. 1980, ApJ, 241, 779
Kitamoto, S., Tsunemi, H., Pedersen, H., Ilovaisky, S. A., & van der Klis, M. 1990, ApJ, 361, 590
Langmeier, A., Sztanjno, M., Hasinger, G., Truemper, J., & Gottwald, M. 1987, ApJ, 323, 288
Lewin, W., van Paradijs, J., & Taam, R. 1993, Space Sci. Rev., 62, 223
Liang, E. P., & Nolan, P. L. 1984, Space Sci. Rev., 38, 353
Machin, G., et al. 1991, MNRAS, 247, 205
Makishima, K., Maejima, Y., Mitsuda, K., Bradt, H. V., Remillard, R. A., Tuohy, I. R., Hoshi, R., & Nakagawa, M. 1986, ApJ, 308, 635
Margon, B., Thorstensen, J. R., & Bowyer, S. 1978, ApJ, 221, 903
Marsh, T. R., Robinson, E. L., & Wood, J. H. 1994, MNRAS, 266, 137
Mason, K. O., Parmar, A. N., & White, N. E. 1985, MNRAS, 216, 1033
Matsuoka, M., et al. 1980, ApJ, 240, L137
Mauche, C. W., & Gorenstein, P. 1986, ApJ, 302, 371
Mitsuda, K., et al. 1984, PASJ, 36, 749
Mitsuda, K., Inoue, H., Nakamura, N., & Tanaka, Y. 1989, PASJ, 41, 97
Miyamoto, S., et al. 1991, ApJ, 383, 784
Nakamura, N., Dotani, T., Inoue, H., Mitsuda, K., & Tanaka, Y. 1989, PASJ, 41, 617
Oda, M. 1977, Space Sci. Rev., 29, 757
Orosz, J. A., & Bailyn, C. D. 1995, ApJ, 446, L590
Orosz, J. A., Bailyn, C. D., McClintock, J. E., & Remillard, R. A. 1996, ApJ, 468, 380
Orosz, J. A., Bailyn, C. D., Remillard, R. A., McClintock, J. E., & Foltz, C. B. 1994, ApJ, 436, 848
Ortolani, S., Bica, E., & Barbuy, B. 1993, A&A, 267, 66
Paczyński, B. 1971, ARA&A, 9, 183
Pan, H. C., Skinner, G. K., Sunyaev, R. A., & Borozdin, K. N. 1995, MNRAS, 274, L15
Parmar, A. N., Angelini, L., Roche, P., & White, N. E. 1993, A&A, 279, 179
Parmar, A. N., Stella, L., & White, N. E. 1986, ApJ, 304, 664
Pavlinsky M., Grebenev, S. A., & Sunyaev, R. A. 1994, ApJ, 425, 110
Pavlinsky, M., Grebenev, S., Finogenov, A., & Sunyaev, R. 1995, Adv. Space. Res., 16, 95
Philips, B. F., et al. 1996, ApJ, 465, 907
Popper, D. M. 1980, ARA&A, 18, 115
Predehl, P., Braeuninger, H., Burkert, W., & Schmitt, J. H. M. M. 1991, A&A, 246, L40
Remillard, R. A., Orosz, J. A., McClintock, J. E., & Bailyn, C. D. 1996, ApJ, 459, 226
Sazonov, S. Yu., Sunyaev, R. A., Lapshov, I. Yu., Lund, N., Brandt, S., & Castro-Tirado, A. 1994, Soviet Astron. Lett., 20, 787
Shahbaz, T., Naylor, T., & Charles, P. A. 1994a, MNRAS, 268, 756
Shahbaz, T., Sansom, A. E., Naylor, T., & Dotani, T. 1994b, MNRAS, 268, 763
Shakura, N. I., & Sunyaev, R. A. 1973, A&A, 24, 337
Singh, K. P., & Apparao, K. M. V. 1994, ApJ, 431, 826
Singh, K. P., Apparao, K. M. V., & Kraft, R. P. 1994, ApJ, 421, 753
Smale, A. P., & Lochner, J. C. 1992, ApJ, 395, 582
Strickman, M., et al. 1996a, in preparation
Strickman, M., Skibo, J., Purcell, E. M. Barret, D., & Motch, C. 1996, A&AS, in press
Sunyaev, R. A., et al. 1988, Soviet Astron. Lett., 14(5), 327
———. 1991a, A&A, 247, L29
———. 1991b, Soviet Astron. Lett., 17(2), 123
———. 1993, A&A, 280, L1
———. 1994, Soviet Astron. Lett., 20(6), 777
Tanaka, Y. 1989, in Proc. 23d ESLAB Symp. (Bologna), ed. J. Hunt & B. Battrick (ESA SP-296), 3
Tanaka, Y., & Lewin, W. H. G. 1995, in X-Ray Binaries, ed. W. H. G. Lewin, J. van Paradijs, & E. P. J. van den Heuvel (Cambridge: Cambridge Univ. Press), 126
Thorstensen, J., Charles, P., & Bower, S. 1978, ApJ, 220, L131
Ubertini, P., et al. 1991, ApJ, 366, 544
van der Klis, M. 1994, ApJS, 92, 511
van Paradijs, J. 1978, Nature, 274, 650
———. 1995, in X-Ray Binaries, ed. W. H. G. Lewin, J. van Paradijs, & E. P. J. van den Heuvel (Cambridge: Cambridge Univ. Press), 536
van Paradijs, J., & McClintock, J. E. 1994, A&A, 290, 133
———. 1995, in X-Ray Binaries, ed. W. H. G. Lewin, J. van Paradijs, & E. P. J. van den Heuvel (Cambridge: Cambridge Univ. Press), 58
van Paradijs, J., & van der Klis, M. 1994, A&A, 281, L17
van Paradijs, J., & Verbunt, F. 1984, in AIP Conf. Proc. 115, High Energy Transients in Astrophysics, ed. S. E. Woosley (New York: AIP), 49
van Paradijs, J., & White N. E. 1995, ApJ, 447, L33
Westerlund, B. E. 1991, in IAU Symp. 148, The Magellanic Clouds and Their Dynamical Interaction with the Milky Way (Dordrecht: Kluwer), 15
White, N. E. 1993, in AIP Conf. Proc., Vol. 308, The Evolution of X-Ray Binaries, ed. S. S. Holt & C. S. Day (New York: AIP), 53
White, N. E., Kaluzienski, J. L., & Swank, J. L. 1984, in AIP Conf. Proc. 115, High Energy Transients in Astrophysics, ed. S. E. Woosley (New York: AIP), 31
Wilson, C. K., & Rotschild, R. E. 1983, ApJ, 274, 717
Yaqoob, T., Ebisawa, K., & Mitsuda, K. 1993, MNRAS, 264, 411
Yoshida, K., Mitsuda, K., Ebisawa, K., Ueda, Y., Fujimoto, R., Yaqoob, T., & Done, C. 1993, PASJ, 45, 605
Zhang, S. N., et al. 1996a, A&AS, in press
———. 1996b, A&AS, in press